SOME ASPECTS OF NUMERICAL MODELING OF TEMPERATURE INCREASE DUE TO ULTRASOUND BEAM IRRADIATION OF RAT LIVER

ELEONORA KRUGLENKO, BARBARA GAMBIN

Institute of Fundamental Technological Research, Polish Academy of Sciences
5B, Pawińskiego St., 02-106 Warsaw, Poland
ekrug@ippt.gov.pl

Some aspects of FEM modeling of hyperthermia, the procedure of tissue temperature rise above 37 ^{o}C inside the living organism, as a treatment modality, are studied. Low intensity focused ultrasound (LIFU) beam has been used as a source of temperature rise in the liver tissue during performed experiments in vitro. The comparison of the FEM model of the corresponding heating process and the experimental results has been presented in [1]. In the paper, the FEM model of heating scheme of the rat liver tissue in vivo irradiated by the same ultrasound transducer is formulated. At first, the existence of blood perfusion is taken into account in the model equation. Secondly, the thermal and acoustical properties, which are the input parameters of the numerical model, are taken from the published data in literature. Here, the size and the intensity of heat sources are modeled in two ways on the basis of acoustic nonlinear equation solutions in 3 layers attenuating medium. We demonstrate how the results of FEM model in the case of in vitro and in vivo heating, depend on the assumed power density of heat sources, as well as on the size of the heated area. The results are compared and discussed. The influence of different models on temperature rise profiles are demonstrated.

INTRODUCTION

The process of temperature elevation in tissues, depending on the degree of tissue heating is widely used in medicine in various therapeutic procedures, namely:

a) physiotherapy – temperature rise of 1–2 °C,
b) therapeutic hyperthermia – heating up to 43 °C,
c) thermal ablation – heating of tissue above the 43–45 °C.

External heat sources inside soft tissues can be produced e.g. by electromagnetic or ultrasound irradiation or by application of electric voltage. The most important advantage of the usage of ultrasound in medical therapy is a therapeutic effect on the localized area inside the body without damaging surrounding tissue. In the paper we deal with the ultrasounds beam generating heat when it is applied to a tissue.

Besides the traditional use of ultrasound in medical diagnostics in case when the effect on living tissue is negligible there is increasing interest to use ultrasound as the activation of processes in different bio-structures (separate cell, tissue, organs) and to obtain the changes in their physical or functional properties.

The focused ultrasound beam of high power (HIFU-therapy) or low power (therapeutic hyperthermia) is used for the heating of living tissue. The mechanism of tissue heating in hyperthermia, physiotherapy, HIFU-therapy is the same: the ultrasonic beam irradiation in the tissue produces the heat as the effect of absorption i.e. conversion of acoustic energy into optical molecular vibrations, which are measured by temperature increase. This oldest and the most widely method is used in the physiotherapy, in the treatment of human diseases of the locomotive apparatus, rheumatic diseases, osteoarthritis.

For physiotherapy ultrasound transducers producing the intensity of 1 W/cm^2 acoustic power are used to heat the tissue no more then 1 °C, meanwhile the exposure time is about 10 minutes.

Therapies using the focused acoustic beam of high intensity (HIFU – High Intensity Focused Ultrasound) are currently the fastest growing area in medical acoustics. With HIFU the field near the transmitter is low and it does not damage the tissue. However, the intensity in the acoustic focus is rather high, i.e. the value of c/a 1000 W/cm^2 is enough to get the significant heating of a tissue. For example, the tissue increases temperatures above 70 °C in a few seconds. The temperature increase above 43 °C initiates a process of intracellular protein denaturation, and it is used in the surgical treatment, which often is called an acoustic ablation or acoustic surgery. Radiofrequency ablation allows an accurate non-invasive ultrasonic damage or destruction of tissue, for example, tumor tissue from cancer. Particulars, HIFU can be used to stop the internal bleeding without damaging surrounding tissue, for example, after the strokes.

In the hyperthermia the ultrasonic beam of low intensity of the order 1–10 W/m^3 (LIFU) irradiating tissue during the 10–60 minutes is used. This provide that the local warming is preserved in the range 40 °C – 43 °C. The temperature increase up to 43 °C starts the heat shock-controlled mechanism, which is the complex biochemical process called HSR (Heat Shock Reaction). The proteins (Heat Shock Proteins, HSP) ‘repairs’ not only such proteins, which are damaged by heat, but also proteins changed in different disease processes. This is the role of HSP’s in gene therapy. If the temperature exceeds 43 °C, then irreversible process of protein denaturation appears. So, during the therapy the temperature should be maintained in the same narrow range of growth and it must be concentrated in the well defined area of tissue. Therefore it is necessary to increase the precision of the prediction of the size of thermal action on biological tissue by defining the parameters of ultrasound beam and duration of its action. It was noted that the effectiveness of both, radiotherapy and chemotherapy, using the hyperthermia in the treatment of cancer, is increasing. Difficulties in monitoring temperature rise in the tissue and its preserving in a fairly narrow range (42–43 °C) still does not manage using the hyperthermia as a standard medical procedure.

In the process of ultrasound therapeutic applications, the validation of numerical prediction must be made in animal experiments performed in vivo. Such experiments are

planned in the Department of Ultrasound IFTR PAS. Independently it is necessary to proceed numerical modeling which allows to calculate the distribution in time and of the space temperature field. Some elements of such a modeling of the tissue heating are presented in this paper.

1. NUMERICAL MODEL

The bio-heat transfer equation (Pennes equation, cf. [1, 2, 3]) for an inhomogeneous medium, occupying an area V in 3 dimensional Euclidean space, has the following form

$$\rho(\mathbf{x})C(\mathbf{x})\frac{\partial T(\mathbf{x},t)}{\partial t} = \nabla \cdot K(\mathbf{x}) \cdot \nabla T(\mathbf{x},t) + Q_p(\mathbf{x},t) + Q_{\text{int}}(\mathbf{x},t) + Q_{ext}(\mathbf{x},t), \quad \text{for} \quad \mathbf{x} \in V, \quad (1)$$

where T, t, ρ, C, K are temperature, time variable, density, specific heat, thermal conductivity of a medium (in general second order tensor), respectively. Here ∇ denotes the gradient operator and the dot '$\cdot$' denotes the contraction operator. The term $Q_p(\mathbf{x},t)$ describes the process of blood perfusion, i.e. cooling or heating caused by the blood flow. The internal heat is produced by chemical processes in tissues (metabolism) and corresponding heat sources are denoted here by $Q_{\text{int}}(\mathbf{x},t)$. The term $Q_{ext}(\mathbf{x},t)$ describes external heat sources introduced to the tissues. In the present model $Q_{ext}(\mathbf{x},t)$ is produced by the focused ultrasonic beam with low intensity. The tissue heating model i*n vitro* was used in [1] with neglected perfusion and internal heat sources, so that

$$Q_p(\mathbf{x},t) = 0, \qquad Q_{\text{int}}(\mathbf{x},t) = 0. \quad (2)$$

In the model for tissue heating *in vivo* we put

$$Q_p(\mathbf{x},t) = w_b C_b (T_b - T), \quad (3)$$

where w_b, C_b are the blood perfusion coefficient and specific heat of blood, T_b denotes the blood temperature in vessels. It is assumed that the perfusion rate w_b is equal 0.9 kg/(m^{3}s), cf. [4, 5]. The heat generation term $Q_{\text{int}}(x,t)$ due to thermal effects of metabolism, we take like in [4], $Q_{\text{int}}(x,t) = 1085$ [W/m^3]. The geometry in the numerical model is shown in Fig. 1, cf. [1, 6].

2. MODELING SOURCE HEAT

Two special numerical approximations of heat sources are considered in this paper. The first case concerns the homogeneous distribution of the heat power density in the area of 3 concentrated cylinders mimicking the real size of the acoustic beam (Fig. 1). Power density of heat sources throughout the heating area is uniform and equal 10^6 [W/m^3], see Fig. 4a. The second case concerns the non-homogeneous distribution of power density. The numerical data used in what follows, have been obtained by courtesy of J. Wójcik from Department of Ultrasounds as a solution of non-linear acoustic wave equation in three layer lossy medium.

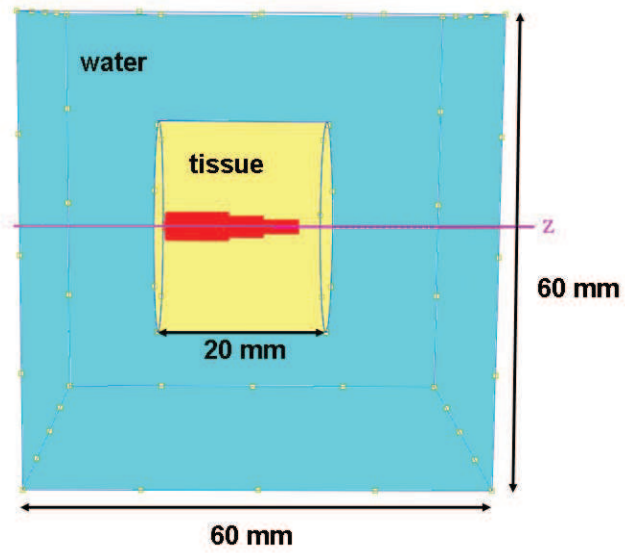

Fig. 1. The form of homogeneous distribution of heat sources assumed in the Model 1, z is the beam axis

Nonlinear acoustic wave propagation in three-layer lossy medium proposed is numerically solved in [7, 8] and the heat sources distribution takes the form:

$$Q_{ext}(\mathbf{x},t) = Q_0 \cdot Q_{ZR}, \tag{4}$$

where Q_{ZR} is 100x50 numerical matrix. Q_{ZR} is shown in Fig. 2, where z is the beam axis. In the case, the dimensional coefficient is assume as $Q_0 = 4{,}713$ [W/m^3].

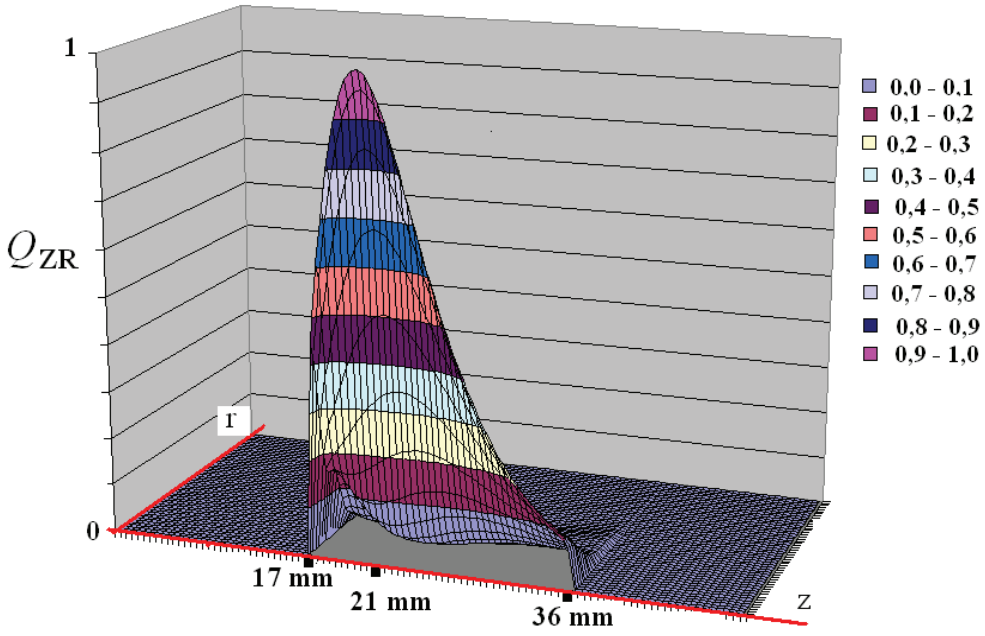

Fig. 2. Heterogeneous distribution of power density for heat sources in cylindrical coordinates (z, r)

We use the above results in the Model 2. We approximate $Q_{ext}(z,r)$ two dimensionless continuous functions as follows

$$Q_0 \cdot Q_{ZR} \approx e^{-1600r} \cdot f(z)\left[\mathrm{W/m^3}\right]. \tag{5}$$

The $f(z)$ is approximated by Padé approximant of the order [3/4] (rational function). We point out that the heat source power decreases exponentially in the direction of the radius, and so we establish that the width of the beam is constant and is equal c/a 0.006 m.

In Fig. 3 the a graph of is depicted. By using method of least squares the

$$\begin{aligned} f(z) = {} & (0{,}3295057927 - 24{,}86480007z + 201{,}5311886z^2 + 6059{,}064437z^3)/ \\ & (1 - 178.5084647z + 1185{,}19464z^2 - 345728{,}8241z^3 + 3666966{,}791z^4) \times 10^6. \end{aligned} \tag{6}$$

The distribution of heat source density in Model 2 is given by formula (5) and depicted in Fig. 4b. In the numerical example, Fig. 4b, the total power of the heat source has been assumed to be equal 0.16 W.

In the next section we compare the calculated in two models distribution of temperature field after 20 minutes of heating with the experiment data, cf. [1].

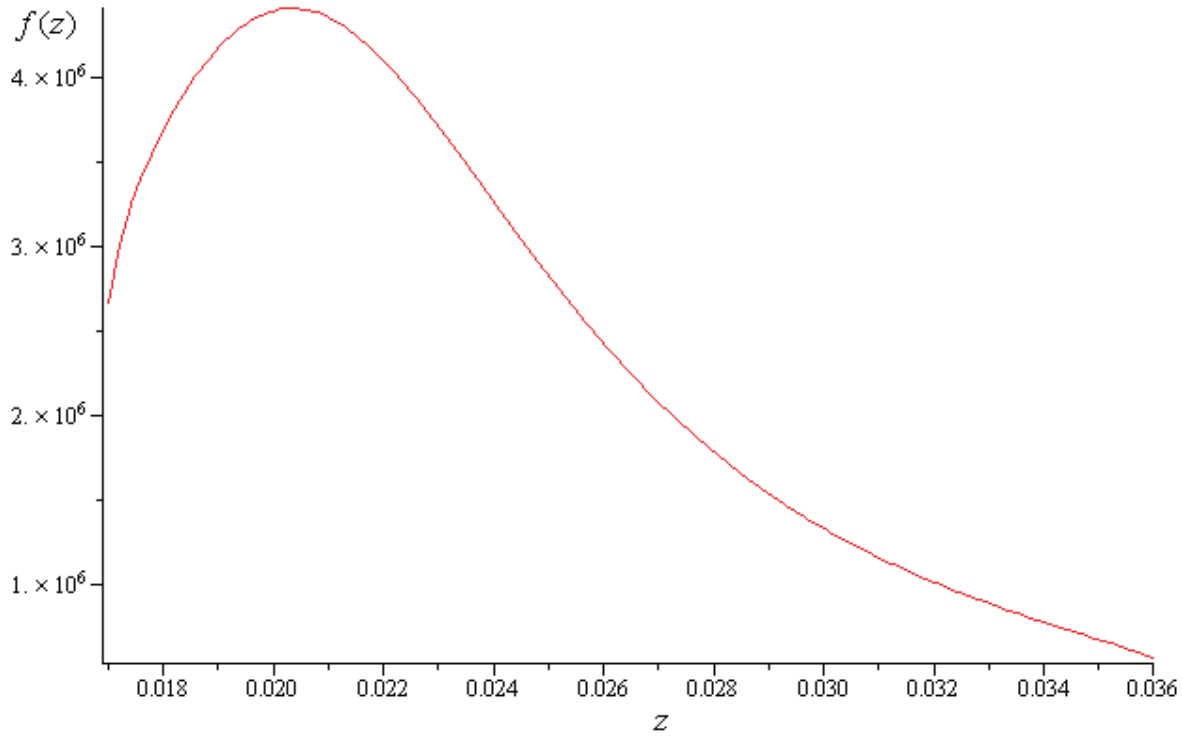

Fig. 3. Graph of the function $f(z)$ given by formula (6)

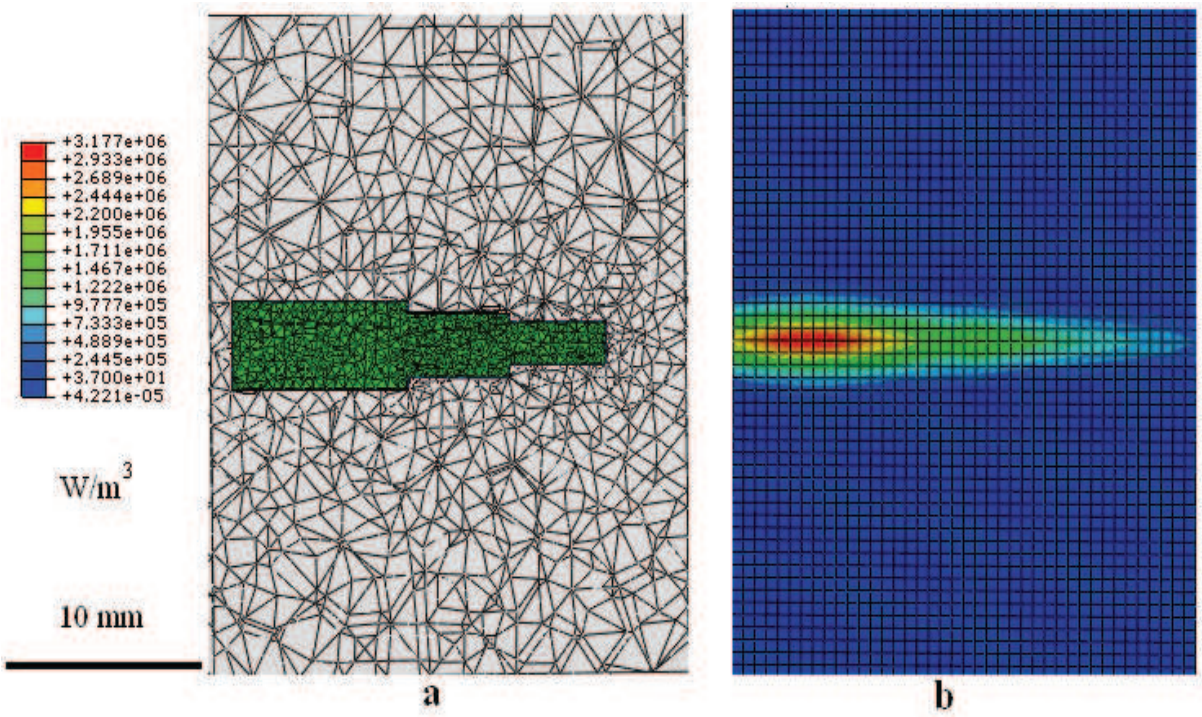

Fig. 4. Distribution of power of heat sources density: a) Model 1, b) Model 2

3. MODELING OF TISSUE HEATING *IN VITRO*

The Abaqus 6.9 software (DS Simulia Corp.) was used in numerical calculations performed with the general model, described in [1]. The initial temperature 37 ^{o}C has been assumed, material parameters for animal liver, water and blood are given in Tab. 1.

Table 1. Material properties of water, tissue and blood

Material	Water	Tissue	Blood
Density $\left[\mathrm{kg/(m^3)}\right]$	1000	1060	1000
Specific heat $\left[\mathrm{J/(kg\ K)}\right]$	4200	3600	3800
Conductivity $\left[\mathrm{W/(m\ K)}\right]$	0.6	0.5	0.6

Firstly, numerical experiments were performed on both models for tissue *in vitro*. Illustrations of the distribution of temperature fields after 20 minutes heating tissue *in vitro* along the beam axis for each model heated area, discrete distribution in Model 1 and continuous in Model 2, are shown in Fig. 5.

Comparing this two models we specify the areas of tissue where the temperature exceeded 43 ^{o}C. The length of the area along the z axis, where the temperature is above 43 ° C for Model 1 is 13.1 mm, for Model 2 is 10.5 mm, the widths across the axis z are 4.5 mm and 3.87 mm respectively.

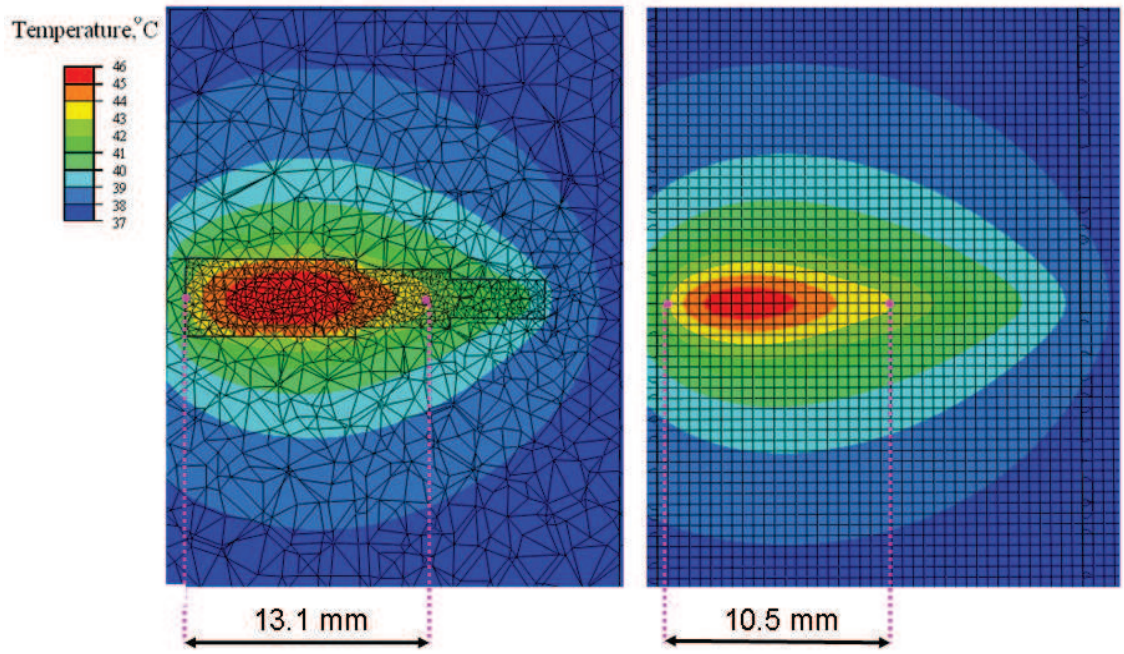

Fig. 5. Comparison of temperature in tissues *in vitro* model along the acoustic beam axis after 20 min irradiation for different models

Temperature rise at the time at various distances from the transducer: 18, 21, 26, 31, 36 mm in Model 1 and Model 2 shown in Fig. 6. We note, that the distance of 21mm along the axis from the transducer is the focal point, the temperature reached at this point is the highest in both models and is nearly identical: in Model 1–45.78 °C, in Model 2–45.79 °C. The differences in other points are of approximately 0.1–1.2 °C, as it is shown in the Fig. 6.

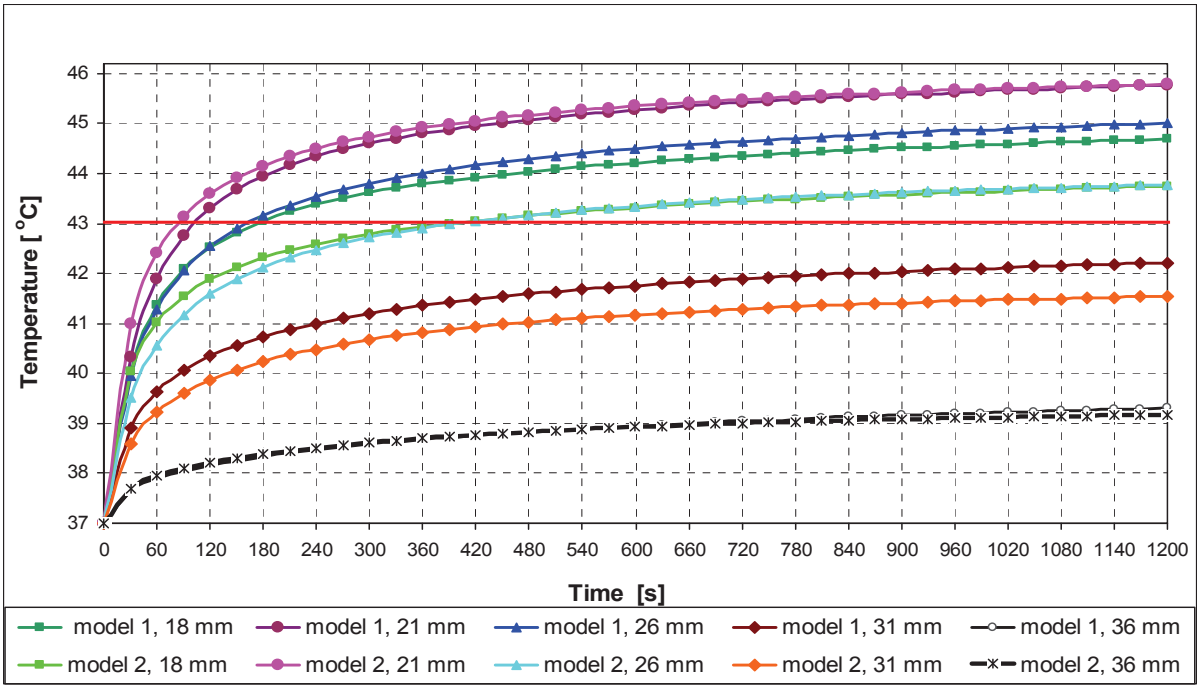

Fig. 6. Comparison of the temperature variation in time predicted by numerical calculation, for Models 1 and 2, at different distances from the transducer

Now, we compare the results of temperature calculations in the Models 1, 2 with the experimental results, cf. [1]. The mail difference between the temperature measured in the experiment and the calculated in Model 1 is located at the distance of 18 mm from the transducer and is equal 5.59 °C. The difference in the temperature measured and calculated in Model 2 at the same location is equal 4.64 ^{o}C. Probably, it is connected with the fact, that we neglected the effect of convection in the water near the tissue boundary. Using the heating of living tissues for therapeutic purposes it is important to preserve the critical temperature value of 43 °C. For this reason the comparison the time necessary to reach this temperature after 20 min heating in two models, see Tab. 2. is done. In the case, Model 1 is more close to experiment results.

Table 2. Comparison of reaching a critical temperature of 43 ^{o}C

	experiment	Model 1	Model 2
Time in [s] to reach of temperature 43^{o}C	149	120	90

Tab. 3 shows the comparison of the temperature calculated in the Model 1 and 2 with experimental results, presented in [1], at different distances from the transmitter after 20 minutes of heating.

Table 3. Comparison of the temperature elevation after 20 minutes heating

Axial distance from transducer in [mm]	18	21	26	31	36
Measure temperature increment in [^{o}C]	39.10	45.76	45.64	43.15	41.61
Numerical result: temperature in [^{o}C], in Model 1	44.69	45.78	45.01	42.22	39.31
Numerical result: temperature in [^{o}C], in Model 2	43.74	45.79	43.78	41.54	39.18

4. MODELING OF TISSUE HEATING *IN VIVO*

Blood perfusion in tissue was modeled as negative volumetric heat sources in the tissue, proportional to the actual temperature increase. This effect is taken into account in the model by including subroutines which is written in Intel Fortran Compiler 11 to the basic program. The temperature rise within 20 minutes is shown for tissue *in vitro* and *in vivo* at different distances from the transducer for Models 1 and 2, respectively in Fig. 7, 8. The differences in tissue temperature increases *in vitro* and *in vivo* are shown in Tab. 4 and 5 for Models 1 and 2 respectively.

The maximum temperature in liver tissue *in vivo* is lower than the 2 °C for Model 1, and 1.7 °C for Model 2 are compared with the calculated temperature for the tissue *in vitro* (see Tab. 4, 5). This result corresponds the preliminary experimental data, received from living rat liver.

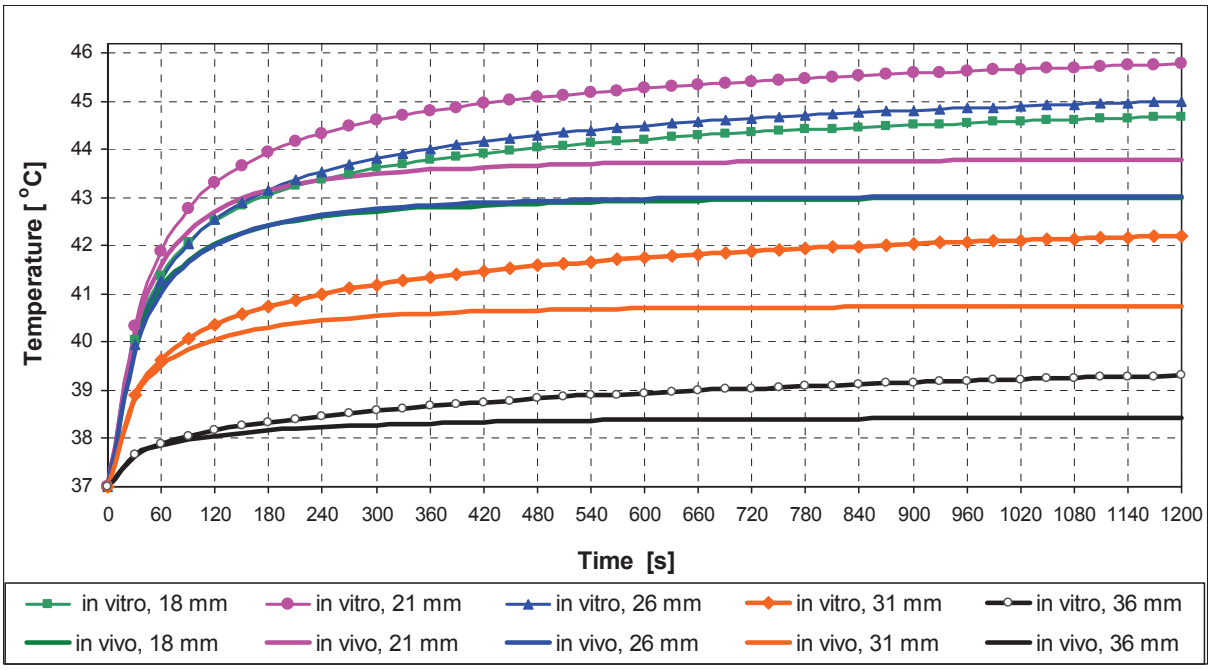

Fig. 7. Comparison of temperature increase during 20 min heating at different distances from the transmitter for the tissue *in vitro* and *in vivo* (including perfusion) for Model 1

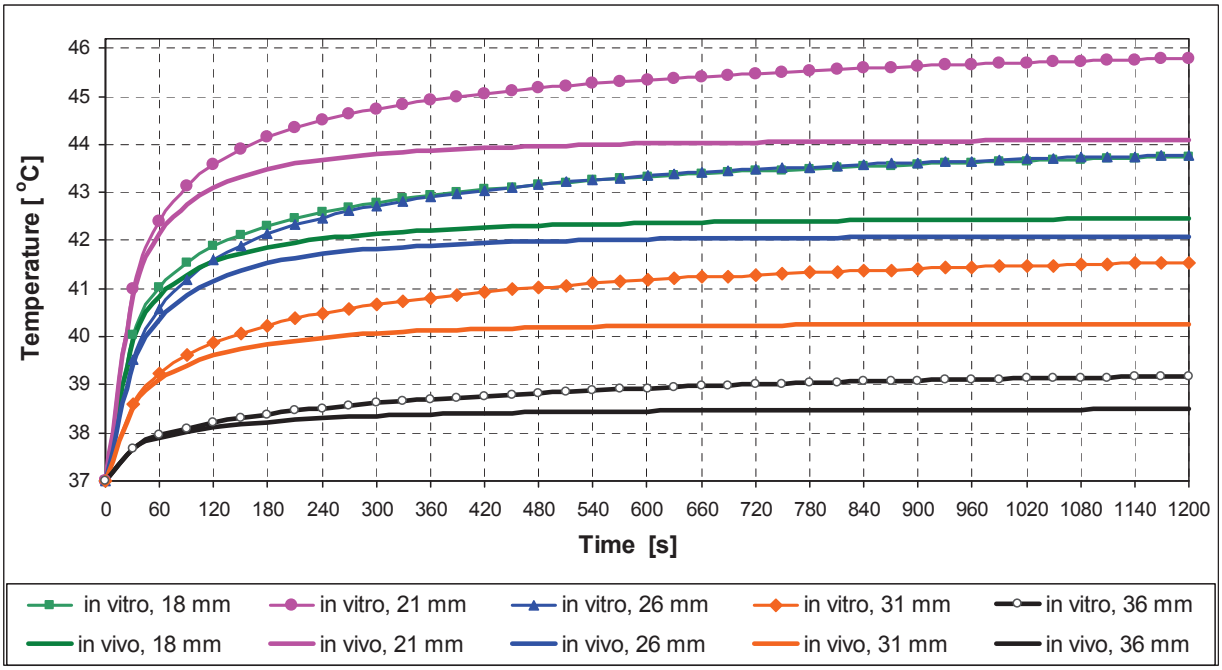

Fig. 8. Comparison of temperature increase during 20 min heating at different distances from the transmitter to the tissue *in vitro* and *in vivo* (including perfusion) for Model 2

Table 4. The temperature increase after 20 minutes heating for tissue *in vivo* and *in vitro* for Model 1

Axial distance from transducer in [mm]	18	21	26	31	36
Numerical result: temperature in [^{o}C], in Model 1 for tissue *in vitro*	44.69	45.78	45.01	42.22	39.31
Numerical result: temperature in [^{o}C], in Model 1 for tissue *in vivo*	43.01	43.79	43.03	40.75	38.43

Table 5. The temperature increase after 20 minutes heating for tissue *in vivo* and *in vitro* for Model 2

Axial distance from transducer in [mm]	18	21	26	31	36
Numerical result: temperature in [^{o}C], in Model 2 for tissue *in vitro*	43,74	45.79	43.78	41.55	39.18
Numerical result: temperature in [^{o}C], in Model 2 for tissue *in vivo*	42.46	44.09	42.09	40.27	38.49

This difference in the results is due to the selection of the shape of the area heating in both models and the selection of the power density of heat source. As a result the temperature rise depends on the shape of the beam of acoustic modeling. Model 2 simulates a more precise phenomenon of further processing of the sound energy into heat. But the computing time for Model 1 is 2 times smaller which may be important in more difficult cases. However such modeling is a complex problem because of the shape of the liver. In this case Model 2 can be more suitable, see Fig. 9.

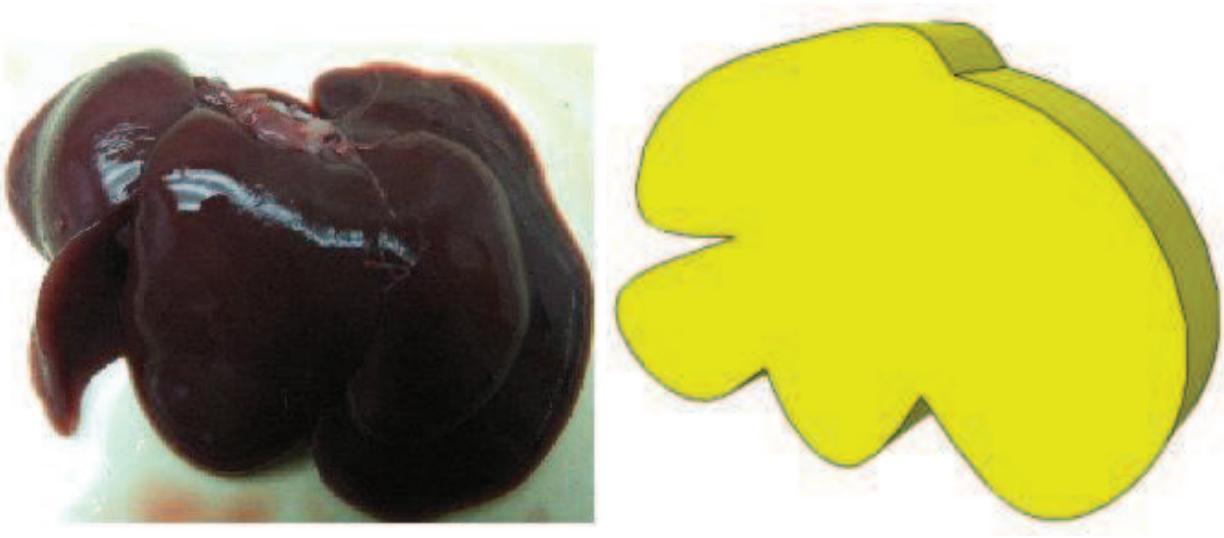

Fig. 9. The rat liver and the shape of rat liver adopted by in numerical modelling

Illustration of the rat liver heating of Model 2 across the beam axis are shown in Fig 10.

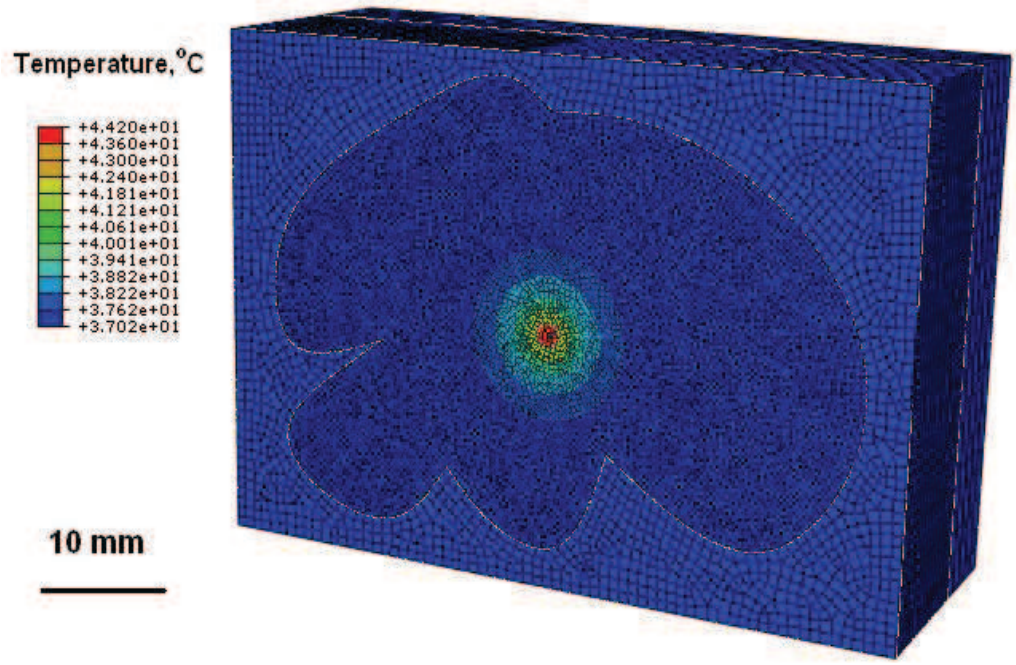

Fig. 10. Temperature pattern in the rat liver across the acoustic beam axis at the axial distance 21 mm from transducer

5. FINAL REMARKS

In the presented models is calculated with the help of FEM. The temperature distribution in the tissue during the irradiation with focused ultrasound beam. The differences between the Model 1 and 2 are due by the shapes of the heating area inside the tissue, as well as, the distribution of intensity of heat sources power in the irradiated region. Comparing Models 1 and 2, we conclude that both models can be used to find the temperature field distribution in the tissue subjected to the heating. Maximum temperature in both models was achieved at a point which lies 21 mm from the transducer. It corresponds to the position of physical focus of the circular transducer and is the same for both models. At other points lying along the beam axis the temperature rise for Models 1 and 2 exhibit differences from 0.1 to 1.2 ^{o}C. The time necessary of reaching the temperature of 43 °C for Model 1, is closer to the experimental time. By contrast, in Model 2, we have the value time of the two times smaller than the time in the experiment. Model 1 is much simpler, less time-consuming and less sophisticated. However, Model 2 is more appropriate to the actual shape of the beam and is useful for the calculation of the tissue heating of any shape. Both models can be used to calculate the temperature field in the tissue *in vivo*, accompanied by the appropriate subroutine. Both this models are also useful to compare a variety of soft-tissue heating process with different physical properties. To make the shape of the rat liver more realistic, we suggest to use the geometry of Model 2. The presented results will be also used to further developing of the fully coupled thermo-acoustical model. The next problem is to take account the changes of properties of the tissue during the irradiation time, and the temperature changes effects on the nonlinearity coefficient, as well as, other acoustic characteristics of the tissue, what in turn will affect the intensity of heat sources and the heating process itself.

ACKNOWLEDGMENTS

This work was partially supported by the Polish ministry of Science and Education, project NN518426936.

REFERENCES

[1] Gambin B., Kujawska T., Kruglenko E., Mizera A., Nowicki A., Temperature Field Induced by Low Power Focused Ultrasound on Soft Tissues During Gene Therapy, Numerical Predictions and Experimental Results, Archives of Acoustics, 34, 4, (2009), 445–459.

[2] Pennes H. H., Analysis of tissue and arterial blood temperatures in the resting human forearm, Journal of Applied Physiology, 1, (1948), 93–122.

[3] Telega J. J., Stańczyk M., Modelling of soft tissues behaviour, Modelling in Biomechanics, Lecture Notes 19, Institute of Fundamental Technological Research, Polish Academy of Science, Warsaw 2005, pp. 191–453.

[4] Yue K., Zhang X., Yu F., An analytic solution of one-dimensional steady-state Pennes' bioheat transfer equation in cylindrical coordinates, Journal of Thermal Science, 13, 3, (2004), 255–258.

[5] Ping Y., Numerical analysis of an equivalent heat transfer coefficient in a porous model for simulating a biological tissue in a hyperthermia therapy, International Journal of Heat and Mass Transfer, 52, (2009), 1734–1740.

[6] Kruglenko E., Gambin B., Numerical modeling of the heating area and heat sources intensities in rat liver in vivo, due to the concentrated ultrasound beam of low intensity, Proceeding of Conference, The 57th Open Seminar on Acoustics (in Polish), Gliwice 2010, pp. 103–106.

[7] Wójcik J., Conservation of energy absorption in acoustic fields for linear and nonlinear propagation, The Journal of the Acoustical Society of America, 104, 5, (1998), 2654–2663.

[8] Kujawska T., Wójcik J., Nowicki A., Temperature field induced in rat liver in vitro by pulsed low intensity focused ultrasound, Hydroacoustics, 13, (2010), 156–162.